



*Citation for published version:*

Ross-Pinnock, D & Mullineux, G 2016, Thermal Compensation of Photogrammetric Dimensional Measurements in Non-standard Anisothermal Environments. in *Procedia CIRP: The 9th International Conference on Digital Enterprise Technology – Intelligent Manufacturing in the Knowledge Economy Era.* vol. 56, Elsevier, pp. 416–421. <https://doi.org/10.1016/j.procir.2016.10.070>

*DOI:*

[10.1016/j.procir.2016.10.070](https://doi.org/10.1016/j.procir.2016.10.070)

*Publication date:*

2016

*Document Version*

Publisher's PDF, also known as Version of record

[Link to publication](#)

*Publisher Rights*

CC BY-NC-ND

## University of Bath

**General rights**

Copyright and moral rights for the publications made accessible in the public portal are retained by the authors and/or other copyright owners and it is a condition of accessing publications that users recognise and abide by the legal requirements associated with these rights.

**Take down policy**

If you believe that this document breaches copyright please contact us providing details, and we will remove access to the work immediately and investigate your claim.

9th International Conference on Digital Enterprise Technology - DET 2016 – “Intelligent Manufacturing in the Knowledge Economy Era

## Thermal compensation of photogrammetric dimensional measurements in non-standard anisothermal environments

David Ross-Pinnock\*, Glen Mullineux

*University of Bath, Claverton Down, Bath, BA2 7AY, United Kingdom*

\* Corresponding author. Tel.: +44 1225-386-052 ; *E-mail address:* [d.r.ross-pinnock@bath.ac.uk](mailto:d.r.ross-pinnock@bath.ac.uk)

### Abstract

Manufacturers are currently facing large volume metrology challenges driven by thermal effects such as variation in refractive index and thermal expansion. Thermal expansion is one of the largest contributors to measurement uncertainty and it can often be difficult to realise the standard 20°C temperature required. The current process for dimensional measurement requires that the temperature is measured at the instrument, and the entire measurement volume is scaled linearly by the same factor. Unfortunately, this assumes that temperatures are uniform all over the measurand, which is seldom the case particularly at large volume scales.

Useful for deformation measurement, photogrammetry is increasingly employed in industry, which in some cases can exhibit uncertainties comparable with the industry standard laser tracker. By measuring temperature more broadly and combining this data with finite element analysis, it is possible to compensate each of these points in 3D space along the X, Y and Z axes. Actively creating challenging metrology conditions with highly localized temperature gradients, and maximum temperatures in excess of 45°C has allowed this approach to be tested. Results show that in many cases it is possible to make localized predictions of displacement within the range of photogrammetric measurement uncertainty.

© 2016 The Authors. Published by Elsevier B.V. This is an open access article under the CC BY-NC-ND license (<http://creativecommons.org/licenses/by-nc-nd/4.0/>).

Peer-review under responsibility of the scientific committee of the 5th CIRP Global Web Conference Research and Innovation for Future Production

*Keywords:* Thermal compensation; large volume metrology; photogrammetry; finite element analysis; Light Controlled Factory

### 1. Introduction

Manufacturing products with increasingly challenging specifications requires dimensional metrology that is capable of providing accurate measurement. One of the largest contributors to measurement uncertainty is thermal effects [1, 2], either due to refractive index variations in air in the case of optical metrology, or more generally, through thermal expansion. This being known, the standard temperature for metrology was defined as 20°C [3]. Temperature-controlled metrology labs are available, however temperature control is not always possible in industry. Particularly at the large volume scale, where products are being assembled over tens

of metres, closely controlling temperature to 20°C is often economically prohibitive or impractical.

Currently, the most common means of solving the problem of metrology at non-standard temperatures is to measure the ambient temperature and scale the entire measurand linearly based upon the co-efficient of thermal expansion for the material. This assumes that the temperature distribution upon the measurand is uniform, which is seldom the case. Temperature gradients have been observed in large volume assembly, integration and test (AIT) environments of 3-5°C. Considering a commonly used aerospace material is aluminium, with a relatively large thermal expansion of around  $23 \mu\text{m}\cdot\text{m}^{-1}\cdot^\circ\text{C}^{-1}$ , measurement uncertainty due to

thermal expansion will accumulate quickly at this scale. Assembly variation is also increased due to this expansion.

A novel method has been created to compensate dimensional measurement for anisothermal non-uniform thermal expansion at non-standard temperatures. This hybrid computational and physical measurement-based approach combines metrology instrumentation with simulation to more accurately predict thermal expansion. Temperature measurement technologies have been identified for use in assembly environments [4] and the body of literature on recent developments pertaining to these technologies has been reviewed [5]. The methodology behind this approach has been outlined [6], which laid the framework for this technique, which is studied experimentally here.

## 2. Measurement Scenarios

### 2.1. Frame structure

A cuboidal frame structure made from aluminium 6063 extruded profile by MiniTec is to serve as the measured object in this study. The frame is made up of 12 individual beam members and fastened together with proprietary MiniTec Powerlock fasteners. Supporting the frame at the bottom are 4 Omnitrac ball transfer units. Four plates adhered to the floor give the ball transfer units a low friction flat surface to run on, allowing for largely unimpeded thermal expansion in three directions. One ball transfer unit is nested in a hole drilled on one of the plates in order to provide constraint. A fiducial post is also used to reset the frame against repeatably, and to constrain yaw rotation of the structure.

### 2.2. Heating method

The ambient temperature of the environment is typically the source of thermal inhomogeneity in industrial assembly environments, meaning that using a convective heating method in the form of a fan heater would be considered a realistic, but exaggerated heating method for this experiment. Two heater settings have been used on a fan heater, and directed toward the frame structure in one corner. This localized heating provides an extreme example which will produce a significant amount of thermal expansion. At this scale in these conditions, the measurement uncertainty of the photogrammetry is of the order of 20  $\mu\text{m}$ , whilst the thermal expansion is likely to be around 200  $\mu\text{m}$  from initial measurements. This order of magnitude difference between measurement uncertainty and thermal expansion will allow variation due to thermal expansion and variation due to measurement uncertainty to be largely separated.

### 2.3. Design of experiments

Measurements are taken at ambient temperature (H0) before each round of heating to get a set of reference coordinates to apply compensation. This should also mitigate any hysteresis effects upon the structure. For each scenario, a single finite element model was used with the measured

temperature data from both of the measurement scenarios and applied as boundary conditions. The first measurement is carried out at heater setting 2, position 1 (H2P1) and the second is carried out at heater setting 1, position 2 (H1P2). Agreement between the measured data and the simulated measurement data is the performance metric for this experiment.

## 3. Metrology

### 3.1. Dimensional metrology (photogrammetry)

Photogrammetry is a dimensional measurement technique that is increasingly used in industry to measure deformation, often in the automotive and aerospace industries. Targets are adhered to the surface of the measurand alongside reference objects such as scale bars and reference crosses. Scale bars provide a calibrated distance measurement between two points and reference crosses set the origin and orientation of the co-ordinate system. Multiple photographs are taken of the scene and Software is used to perform the bundle adjustment between each of the images and turns the measured targets into 3D co-ordinates by finding the centre of an ellipse present in the images. Images are captured exclusively in greyscale and targets are black and white to provide reproducible contrast. Software also uses RGB colour values to recognise these. Coded targets can also be used which have specific patterns that are recognised by the software to represent a point.

The Aicon DPA system used here is formed of a modified Nikon 3dx digital single lens reflex (DSLR) camera equipped with a 28 mm Nikkor prime lens. A hot-shoe-mounted flash with built-in diffuser illuminates the scene. Captured images are sent directly to a laptop computer via local Wi-Fi connection. Aicon 3D Studio software running on the laptop is used to perform the measurement and is also used for analysis of measurement data.

The Aicon DPA system was used to take measurements of the frame in each of the scenarios. With free-roaming handheld photogrammetry, a lot of the measurement capability comes from the images being captured from a wide range of angles and elevations. Fig. 1. shows the various

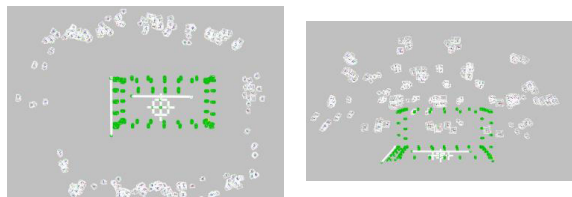


Fig. 1. Example image illustrating variety of vantage points used during photogrammetric measurement from the a) top view and b) side view

camera positions that were used during measurement. At each position, images are captured in portrait and landscape. Around ten vantage points were used with the photographer stood on the floor, from which photographs were taken at both standing and crouching positions. The frame stands at little

over 1 metre high, therefore a ladder was required to capture further images of the frame from above. Eight ladder vantage points were used from two different heights at each position. Due to the available space around the structure, full coverage was difficult to achieve however this plan allowed this to be largely mitigated. In some cases points were difficult to measure and so further images had to be captured. In total between 200 and 250 images were typically taken for each measurement over a period of 15-30 minutes.

### 3.2. Temperature measurement

An FLIR handheld infra-red (IR) thermal imaging camera allowed the temperature distribution on the frame to be recorded when the fan heater was running during the four different measurement scenarios. The manufacturer's stated accuracy for the IR camera is  $\pm 2^\circ\text{C}$  meaning the usefulness of

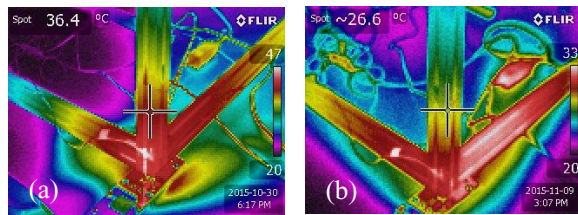


Fig. 2. Thermal images for the heated corner of the frame for (a) heater setting 2, position 1; and (b) heater setting 1, position 2.

the camera from the perspective of quantitative thermography is somewhat limited compared to invasive sensors. Conversely the sensitivity of the camera is good, at  $<0.045^\circ\text{C}$ , meaning that when combined with their imaging capability, they can provide useful qualitative measurements in anisothermal environments.

Using the IR thermal images in a qualitative capacity was useful in deciding where invasive temperature sensors needed to be positioned. As the heating was highly localized, the sensor density in the corner in which the fan heater was situated was increased, with sensors at the other end of the frame being relatively sparse. One temperature sensor (one type T thermocouple referred to as TC0) was used to monitor the ambient temperature at one position. This ambient temperature was taken just above one of the granite slabs. The sensor was free to air however was partially shielded to reduce noise resulting from erratic airflow on the sensor. The further twelve type T thermocouples were used to cover the rest of the frame. Around the point of heating, four Omega thin film platinum resistance temperature detector sensors (RTDs) were used to increase the sensor density.

## 4. Computational thermal compensation

### 4.1. Temperature measurement

Finite element analysis (FEA) was used to simulate the resulting thermal expansion of the MiniTec frame under the thermal load from the fan heater. A CAD model of the frame was constructed specifically for the simulation. The MiniTec

profile was simplified to remove the chamfers and fillets to allow for fewer mesh elements to be used. Fig. 3. shows a side-by-side comparison of the original (a) and simplified (b) CAD model cross-sectional profiles. Each of the dimensions used in the CAD model of the frame were assumed to be nominal.

From the level of stability seen in the four heating profiles of each scenario (see section 3.2.3), an assumption was made that if the temperature was this stable, a steady-state thermal

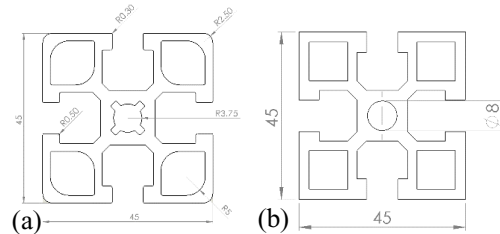


Fig. 3. (a) Original cross-section within the CAD model; (b) simplified CAD model cross-section.

analysis might be an appropriate means of modelling thermal expansion of the MiniTec frame.

Boundary conditions averaged over the course of the dimensional measurement from each of the temperature sensors were applied to the 4 nearest nodes on the mesh to the corresponding sensor position.

Convection and radiation losses in this case were not added to the model because the temperature sensor measurement would have included this cooling effect. Instead, using the conductive properties of the material, the overall temperature distribution was calculated from these discrete temperature sensor points.

Importing the material data, geometry and temperature distribution result from the thermal analysis into the static structural analysis allowed the thermal expansion to be simulated.

As illustrated in Fig. 4., a coarse mesh was used in this instance in order to improve computation time as a shorter simulation time would be preferred in industrial applications.

Fig. 5. shows the constraints and loads applied to the static structural analysis, in addition to the temperature distribution calculated during the thermal analysis. Normal earth gravity was applied in the  $-Y$  direction (downward vertically) upon the frame. The frame was supported at the ball transfer units using a displacement constraint, in which the ball transfer

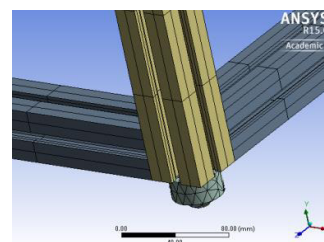


Fig.4. Rendering of the coarse finite element mesh at one corner of the frame.

units were free to move in the X and Z axes but were constrained from moving in the Y direction. Whilst in reality there would have been some level of friction, in this case friction has been omitted from the model. A nodal displacement constraint was placed upon the node nearest to the fiducial post that located the frame and constrained yaw rotation about the Y axis. Displacement solutions in X, Y and Z were found using this method, alongside the total deformation.

The compensation would be achieved by adding the displacement solutions in X, Y and Z to the original reference co-ordinates measured at ambient temperature. In order to do this however, some transformation was required in order to ensure that the co-ordinate systems of the physical dimensional measurement and the simulation from the FEA were aligned. Alignment is the most important aspect of the process as the displacements are relative so the co-ordinate systems will only be sensitive to angular pitch, roll and yaw error. In this case only agreement between measurement and simulation is presented to give an indication of how much of the thermal expansion error can be compensated. **N.B – The simulation and measured co-ordinate system are rotated 90 degrees about the X axis, with the measurement Z axis being vertical, corresponding to the Y axis in the simulation.**

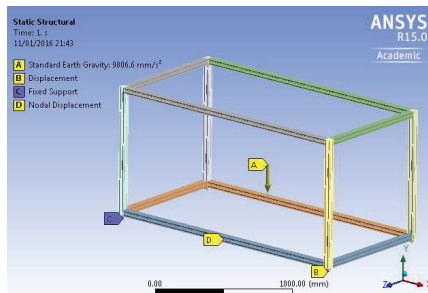


Fig.5. CAD rendering of the structural loads in the finite

The co-ordinate system in the measurement was set by fitting the XY plane to three points on the plates that support the frame: 251, 252, 263. The Z axis was aligned to point 354 and the X axis intersected targets 353 and 425. The targets about the fixed corner of the frame were used for best-fitting of the ambient and heated measurements (101, 106, 111, 112, 129, 354). Measuring in the expansion of points along the X axis was achieved by measuring the distance along the axis from the fixed corner targets to target 425. Y was measured along the axis from targets 134, 82, 114 and 425 to target 268. Finally, expansion in Z (vertical) was measured from targets 134, 82, 114 and 425 to target 138.

## 5. Results and discussion

### 5.1. Measurement and deformation analysis

Measurement of the frame was carried out in the manner outlined and deformation analysis within the Aicon 3D Studio software was performed to quantify the displacement of the

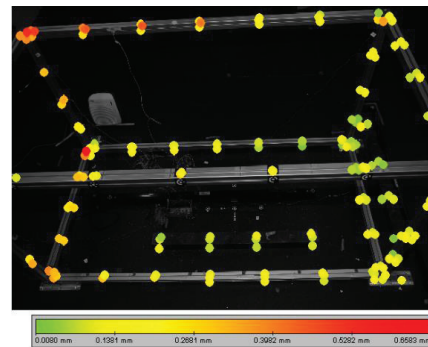


Fig. 6. Example photograph captured during the photogrammetric measurement overlaid with target total deformation.

various points. Fig. 6. shows an example of the photogrammetry scene with the measured targets overlaid onto one of the captured images. The heater is pictured in the top-left hand corner of the image. The total deformation is

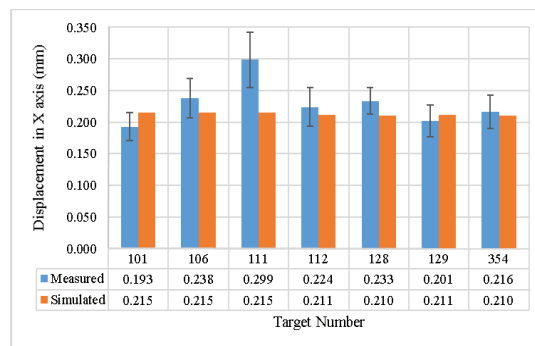


Fig. 7. Graph showing the measured displacement in the X axis compared to the simulated prediction.

illustrated by the colour coding at each of the targets. Measured displacements in the X, Y and Z axes are shown from Fig. 7. to Fig. 12. in blue.

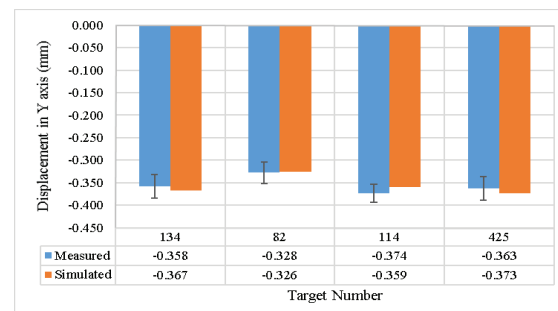


Fig. 8. Graph showing the measured displacement in the Y axis compared to the simulated prediction.

### Measurement 1 - heater setting 2, position 1

Fig. 7. shows the displacement against the measured displacement in the X axis to point 425. A significant amount

of thermal expansion can be predicted using this basic simulation approach and the majority of the points lie within the measurement uncertainty of the photogrammetry system as shown by the error bars. In the X axis there was an average measured displacement of 229 ( $\pm 0.29 \mu\text{m}$ ), with the simulation returning an average displacement of 212  $\mu\text{m}$ . Displacement in the Z axis proved to be the most difficult to predict, with only 293  $\mu\text{m}$  of the measured displacement of 417  $\mu\text{m}$  ( $\pm 29 \mu\text{m}$ ). It is possible that the number of sensors on the shorter beam opposite the heater is insufficient to capture the full range of temperatures present in order to accurately predict the expansion in this direction

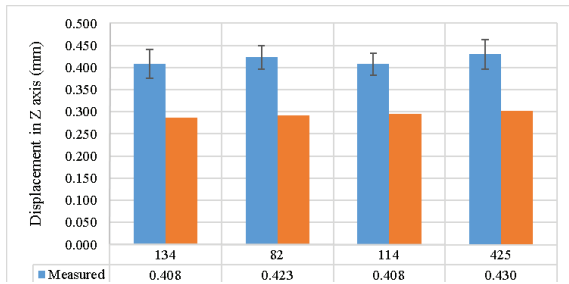


Fig. 9. Graph showing the measured displacement in the Z axis compared to the simulated prediction.

Measurement 2 - heater setting 1, position 2

In Fig. 10. the displacement in the X axis for the lower heater setting is around 90  $\mu\text{m}$  less than that observed in the first measurement scenario, on average. Whilst there was more disparity in individual targets, the average displacement in X was around 144  $\mu\text{m}$ , compared to the average prediction of 141  $\mu\text{m}$ . Target 111 again seems to have moved a lot more than the other points in both scenarios, which is explained by the fact that it is furthest away from point 425 and is placed

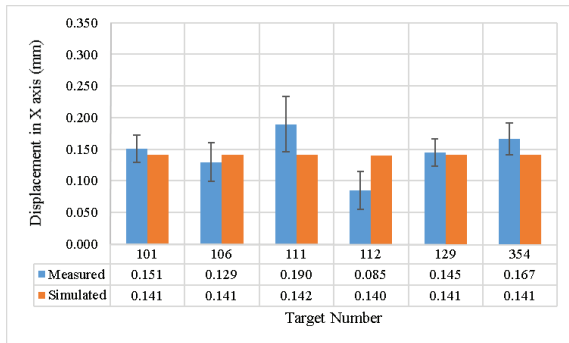


Fig. 10. Graph showing the measured displacement in the X axis compared to the simulated prediction for H1P2.

upon the short, 1 metre long beam at the far side. Simulations and measurement show that the bottom corner pictured in Fig. 6. is forced in the opposite direction due to the expansion in the adjacent 2 metre long beam.

Displacement in the Y axis to point 268 was measured to be 195  $\mu\text{m}$ , as shown in Fig. 11. The FEA prediction appeared to underestimate the thermal expansion in this scenario at 156  $\mu\text{m}$  on average. One of the problems with this type of simulation is that there is the possibility in more compliant structures such as this for the frame to stray from the coordinate system via rotation, making it more difficult to make on-axis predictions. Measurements between the points on the XY plane however give displacement of 150  $\mu\text{m}$  on

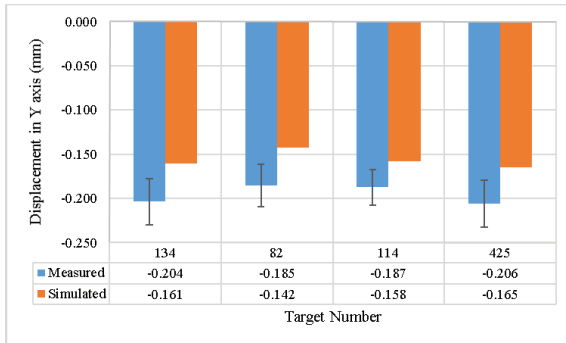


Fig. 11. Graph showing the measured displacement in the Y axis compared to the simulated prediction.

average.

The prediction of Z displacement as shown in Fig. 12. appears to underestimate the vertical thermal expansion. The average measured displacement in Z is measured to be 221  $\mu\text{m}$ , whereas the average prediction is 125  $\mu\text{m}$ . Looking at the X displacement to target 138, the measured displacement is 226  $\mu\text{m}$ , which is good, compared to a prediction of 235  $\mu\text{m}$ . Once more it does appear that there has been some rotation as the straight-line prediction for the expansion in Z to target 138 is 210  $\mu\text{m}$ . This is encouraging as this means that the model is predicting the expansion reasonably accurately but further work needs to be done on reproducibly aligning the measured and simulated geometries in order to produce fully compensated measurements using reference coordinates and temperature data.

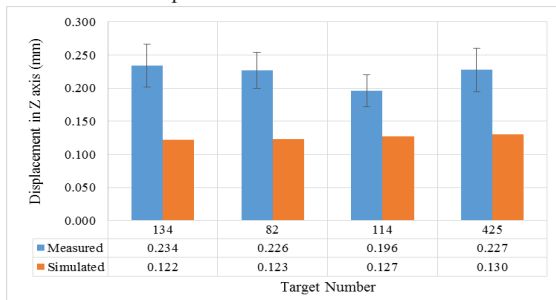


Fig. 12. Graph showing the measured displacement in the Z axis compared to the simulated prediction.

6. Conclusions

Making accurate dimensional measurements for 3D coordinates can be difficult in anisothermal scenarios which can

be hard to avoid in some situations. This paper has outlined and shown the application of a straightforward methodology for two things, the first being temperature measurement for dimensional metrology, which is currently often only carried out on the ambient temperature at the instrument. Finite element simulation of displacement allows for compensation of co-ordinates that would not be possible using current linear scaling methods, due to the presence of highly localized heating.

Using even a simplified finite element model can give predictions that are predominantly within the range of dimensional measurement uncertainty to subsequently allow for the compensation of 3D points.

Cases where there is underestimation of thermal expansion observed in the vertical Z direction could be remedied by providing temperature further inputs to the simulation, and by increasing the model complexity. The example presented made use of simplified geometry, connections and a coarse mesh.

Work in the area of temperature measurement planning is likely to provide an answer to improving the inputs to the simulation and therefore improving predictions. Similarly, work is being done to identify methods in the application of volumetric interpolation of temperature data to feed into the finite element analysis.

Adapting the geometry of the structure so that this matches in both measurement and simulation is important for compensation of 3D points in each of the axes. Methods to employ this kind of geometry correction to improve predictions once the limitations of the finite element analysis are reached is also being explored.

## Acknowledgements

This work was funded by the EMRP Project IND53. The EMRP is funded by the EMRP participating countries within EURAMET and the European Union. We also wish to thank the Department of Mechanical Engineering at the University of Bath.

## References

- [1] Estler WT, Edmundson KL, Peggs GN, Parker DH. Large-Scale Metrology – An Update. *CIRP Annals - Manufacturing Technology*. 2002;51(2):587-609.
- [2] Maropoulos PG, Muelaner JE, Summers MD, Martin OC. A new paradigm in large-scale assembly—research priorities in measurement assisted assembly. *Int J Adv Manuf Technol*. 2014;70(1-4):621-33.
- [3] BSI. BS EN ISO 1. Geometrical product specifications (GPS). Standard reference temperature for the specification of geometrical and dimensional properties. BSI; 2015.
- [4] Ross-Pinnock D, Maropoulos PG. Identification of Key Temperature Measurement Technologies for the Enhancement of Product and Equipment Integrity in the Light Controlled Factory. *Procedia CIRP Special Edition for 8th International Conference on Digital Enterprise Technology - DET 2014 – Disruptive Innovation in Manufacturing Engineering towards the 4th Industrial Revolution*, DOI: 10.1016/j.procir.2014.10.019; 2014 25/03/2014 - 28/03/2014; Elsevier.
- [5] Ross-Pinnock D, Maropoulos PG. Review of industrial temperature measurement technologies and research priorities for the thermal characterisation of the factories of the future. *Proceedings of the Institution of Mechanical Engineers, Part B: Journal of Engineering Manufacture*. 2015.
- [6] Ross-Pinnock D. Integration of Thermal and Dimensional Measurement – A Hybrid Computational and Physical Measurement Method. 38th MATADOR Conference; 28-30th March 2015; Huwei, Taiwan: The University of Manchester; 2015. p. 471-8.